DRELL-YAN PROCESSES IN NUCLEAR TARGETS*

By T. Chmaj

Institute of Physics, Jagellonian University, Cracow** and Institute of Nuclear Physics, Cracow

and K. J. Heller

Institute of Physics, Jagellonian University, Cracow**

(Received September 20, 1984)

The effects of changes of quark distributions inside nuclei, as given by different models of the EMC effect, on the pion-induced cross section for the Drell-Yan process are investigated. The predictions of different models are consistent with each other and indicate visible changes in the cross section, as compared to the naive expectations.

PACS numbers: 13.75.Gx, 25.80.Hp

1. Introduction

The measurement of the EMC effect [1], i.e. the difference between the structure function measured on iron and deuterium, confirmed later for other nuclear targets [2–3], resulted in a multitude of different theoretical explanations [5–18]. All models explaining this effect can be expressed in terms of the change of quark densities inside nuclei as compared to those of free nucleons. This change should manifest itself in other processes, where quark densities are of importance. The simplest to analyze seems to be the Drell-Yan process.

In this paper we continue our work [19] on effects of those differences on the cross section for the Drell-Yan process on nuclear target. We investigate the predictions of different models (which give almost the same results for the EMC effect) for that process. Possible differences in these predictions could help to distinguish between models and invalidate some of them.

The point is, that the knowledge of the electromagnetic structure function F_2, measured in DIS, does not determine separate quark distributions, but only their combinations. Thus it is possible, at least in principle, that the models which give almost identical curves for the EMC ratio give different predictions for the Drell-Yan.

* Work supported in part by the M. Skłodowska-Curie Foundation, Grant No F7-071-P.

** Address: Instytut Fizyki UJ, Reymonta 4, 30-059 Kraków, Poland.

Our paper is organized as follows: in the next Section we present formulae used for calculation of the cross section for the Drell-Yan process. In Section 3 different models of quark structure of nucleus are described. Numerical results for the cross sections derived from abovementioned models are discussed in Section 4. Our conclusions are summarised in the last section.

2

We are considering massive lepton pair production in hadron-hadron collisions by quark-antiquark annihilation (i.e. the Drell-Yan process [20]). Using the standard model [21] we obtain the following formula for the cross section:

$$\frac{d\sigma}{dx_1 dx_2} = K \frac{\sigma_0}{x_1 x_2} N_{q\bar{q}}(x_1, x_2), \tag{1}$$

where: x_i — momentum fraction of (anti)quark in the i-th hadron; $\sigma_0 = \frac{4\pi\alpha^2}{3s}$; s—CM energy momentum squared; K — constant, so-called K-factor;

$$N_{q\bar{q}}(x_1, x_2) = \tfrac{1}{3} \sum_{i=u,d,s} e_i^2 [q^b(x_1)\bar{q}^T(x_2) + \bar{q}^b(x_1) q^T(x_2)]; \tag{2}$$

e_i — charge of i-th quark; $(\bar{q})q$ — (anti)quark density; b — beam; T — target.

$N_{q\bar{q}}$ can be understood as the probability of finding any quark-antiquark pair with momentum fractions x_1, x_2 respectively.

Formulae (1), (2) we obtained in the simple parton model. QCD corrections to this model lead to Q^2-dependence of quark distributions [22] and multiplication of the whole formula by a very weakly x_1, x_2 dependent factor [23].

If we want to investigate the quark distributions inside nucleus by means of $q\bar{q}$ annihilation we shall use a beam which enables us to concentrate on the target. This is easy to achieve for the pion beam, where we have valence antiquarks. In the case of proton beam antiquarks are present in the sea only. As sea quark densities are not well known, the analysis of Drell-Yan process is less conclusive.

Due to the presence of valence antiquark we can neglect the sea of a pion, thus obtaining for the pion beam:

$$\begin{aligned} N_{q\bar{q}}^{\pi^-}(x_1, x_2) &= \bar{u}^{\pi^-}(x_1) \left[\tfrac{4}{9} u_v^T(x_2) + \tfrac{5}{9} s^T(x_2)\right], \\ N_{q\bar{q}}^{\pi^+}(x_1, x_2) &= \bar{d}^{\pi^+}(x_1) \left[\tfrac{1}{9} d_v^T(x_2) + \tfrac{5}{9} s^T(x_2)\right]. \end{aligned} \tag{3}$$

Bearing in mind that $\bar{u}_v^{\pi^-} = d_v^{\pi^-} = \bar{d}_v^{\pi^+} = u_v^{\pi^+}$ from (2) and (3) we obtain for the ratio $R^{\pi^\pm} = \left[\frac{1}{A_1}\left(\frac{d\sigma}{dx_1 dx_2}\right)^{\pi^\pm}_{A_1} \Big/ \frac{1}{A_2}\left(\frac{d\sigma}{dx_1 dx_2}\right)^{\pi^\pm}_{A_2}\right]$ (A_1, A_2 denote number of nucleons inside target nucleus):

$$R^{\pi^-} = \frac{4u_v^{A_1}(x_2) + 5s^{A_1}(x_2)}{4u_v^{A_2}(x_2) + 5s^{A_2}(x_2)}, \qquad R^{\pi^+} = \frac{d_v^{A_1}(x_2) + 5s^{A_1}(x_2)}{d_v^{A_2}(x_2) + 5s^{A_2}(x_2)}. \tag{4}$$

Because of the factorisation which has occured in (3) the ratios given in (4) are only x_2 dependent and we do not have to take into account the structure function of a pion. It is also clearly seen from (4) that for an isoscalar target for the region of $x_2 > 0.3$ (i.e. the region where sea can be neglected) ratios for π^- and π^+ beams are equal.

In the abovementioned calculations we assumed that the so-called K-factor is A-independent. This assumption seems to be a realistic one [24]. Even when it is false it means only that some constant multiplicative factor is introduced in (4), which changes the overall scale but by no means affects the relations between predictions of different models.

In order to avoid this assumption, we consider also the ratio $\left(\frac{d\sigma}{dx_2}\right)_A^{\pi^+} \Big/ \left(\frac{d\sigma}{dx_2}\right)_A^{\pi^-}$. According to (1) and (3) the formula for this ratio is as follows:

$$\frac{\left(\frac{d\sigma}{dx_2}\right)_A^{\pi^+}}{\left(\frac{d\sigma}{dx_2}\right)_A^{\pi^-}} = \frac{d_v^A(x_2)+5s^A(x_2)}{4u_v^A(x_2)+5s^A(x_2)}. \tag{5}$$

3

In this section we reviev briefly different models of the EMC effect proposed recently.

3.1. Furmański and Krzywicki [5]

Krzywicki was first to suggest [4] a possible deviation from a conventional picture of a nucleus as an additive collection of almost free nucleons. The idea presented in that paper was pursued recently in Ref. [5]. The authors state that for the interactions which probe the nucleus during very short time (DIS, high p_T productions) the target should be regarded as an ensemble of instantaneously uncorrelated quarks and gluons rather than a sum of nucleon bags. Applying Kuti-Weisskopf model [25] to the whole nucleus they calculated quark distributions and structure functions. It is worth mentioning that when using this procedure for the deuterium one obtains quite large corrections as compared to the picture of deuterium as a sum of free nucleons.

This model yields only a qualitative agreement with the EMC data. It is, however, interesting to observe that such extreme view of nucleus yields relatively good results.

3.2. Close, Jaffe, Roberts and Ross [6–8]

Another point of view is presented by Close, Jaffe, Roberts and Ross [6–8]. They argue that the scale of quark confinement can change depending on the nucleus. This leads to the increase of the effective size of the nucleon inside nucleus. As a consequence, when analysing for instance DIS one has to take into account, besides the external scale given by the momentum transfer of the process (Q^2), also the internal scale, connected with the confinement scale, which is different for different targets. QCD analysis of these scales leads to the following result [7]:

$$F_2^A(x, Q^2) = F_2^N(x, \xi Q^2), \tag{6}$$

where F_2^A, F_2^N are the electromagnetic structure functions of a nucleon in a nucleus and the free nucleon respectively; ξ — weakly Q^2-dependent factor, given by the ratio of confinement scales (i. e. by the ratio of effective nucleon sizes).

The authors used a simple model in order to calculate the effective size of nucleon inside nucleus. This enabled them to predict the magnitude of the EMC effect as a function of A. We assume that equation (6) holds also for quark distributions.

The idea outlined above is appealing, but unfortunately the agreement with experimental data is not very good.

3.3. Levin and Ryskin [9]

The idea of the increase of the size of the nucleon inside nucleus is the base of the model presented in Ref. [9]. It is easy to formulate this model in the framework of the bag model. As the mass of the bag is proportional to $1/R$, one obtains the following relation between masses and radii of the bags:

$$\frac{m^*}{m} = \frac{R}{R^*}, \tag{7}$$

where * denotes quantities inside nucleus.

DIS occu s on a single bag of a mass m^*, leading to the rescaling of the Bjorken variable

$$x_B^* = \frac{m}{m^*} x_B. \tag{8}$$

From (8) one obtains the following expressions for the structure function:

$$F_{2v}^{N*}(x) = F_{2v}^N\left(\frac{R_N^*}{R_N} x\right) \tag{9}$$

and the quark densities:

$$q_v^*(x) = \frac{R_N^*}{R_N} q_v\left(\frac{R_N^*}{R_N} x\right). \tag{10}$$

The abovementioned formulae are not valid for the sea. The authors take the following expressions for the sea contribution:

$$q_{sea}^*(x) = \kappa q_{sea}(x), \tag{11}$$

where $\kappa = R_N/R_N^* + (R_N^*/R_N - 1)/\langle x_{sea}\rangle$ is calculated from the energy conservation law.

This model is in agreement with the data for $x < 0.6$.

3.4. Dias de Deus [10]

The main assumption of this [10] and many other models [11] is that a nucleus consists not of ordinary nucleons only but also of $3i$ quark clusters ($i = 2, 3, \ldots$). Thus the full description takes into account all possible cluster partitions with appropriate probabilities.

Instead of doing this the author treats nucleus as if it was made of clusters of $\langle i\rangle$ nucleons, $\langle i\rangle$ being the average number of nucleons per cluster (for iron he obtained $\langle i\rangle = 1.08$). This rescales the x variable: $x \to x/\langle i\rangle$.

He uses the quark distributions with standard parametrisation:

$$xV_{\langle i\rangle}(x) = \frac{3\langle i\rangle}{B(\alpha_{\langle i\rangle}, \beta_{\langle i\rangle}+1)}\left(\frac{x}{\langle i\rangle}\right)^{\alpha_{\langle i\rangle}}\left(1-\frac{x}{\langle i\rangle}\right)^{\beta_{\langle i\rangle}},$$

$$xS_{\langle i\rangle}(x) = s_{\langle i\rangle}\left(1-\frac{x}{\langle i\rangle}\right)^{T_{\langle i\rangle}-1}. \tag{12}$$

The parameters $s_{\langle i\rangle}$, $T_{\langle i\rangle}$, $\alpha_{\langle i\rangle}$, $\beta_{\langle i\rangle}$ satisfy the following constraints:
— the number of sea quarks per nucleon is the same as in free nucleon,
— the fraction of momentum carried by valence quarks and sea quarks is the same as in free nucleon.

This model gives correct description of the data for $x > 0.3$. The recent version of the model [10] combines quark clustering effects with those described by Close et al. [7–8]. This version describes the data well in the whole range of x.

3.5. Dominguez, Morley and Schmidt [12]

In the model presented by Dominguez, Morley and Schmidt [12] it is assumed that a nucleus consists of protons and neutrons which properties are however modified by mutual strong interaction. DIS of a lepton is with a good accuracy described by the diagram in Fig. 1. The lepton scatters from a single off-mass-shell nucleon with momentum k which due to the influence of nuclear medium behaves as if it had an effective mass different from the physical nucleon mass. This leads to the following expression for the electromagnetic structure function:

$$F_{2A}(x, Q^2) = A\int_{x^1}^{1} dy d^2k_T G_{N/A}(y, \vec{k})\tilde{F}(x_A/y, Q^2, k^2), \tag{13}$$

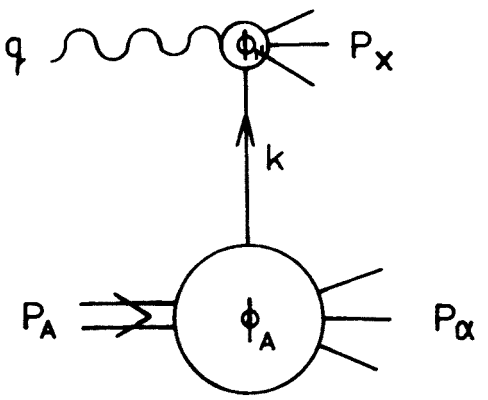

Fig. 1. Diagram of a deep inelastic lepton scattering off a nucleus, as assumed in Ref. [12]

where y is momentum fraction of nucleus carried by a struck nucleon. $G_{N/A}(y, \vec{k})$ describes the distribution of nucleons inside nucleus and $\tilde{F}_{2N}(x, Q^2, k^2)$ is the off-shell nucleon structure function. The authors assumed that it is given by a product of the on-shell structure function and a nucleonic form factor:

$$\tilde{F}_{2N}(x, Q^2, k^2) = f_N^2(k^2) F_{2N}(x, Q^2). \tag{14}$$

The function $G_{N/A}(y, \vec{k})$ is determined by the relativistic nuclear wave function and has been studied in the past [26].

This model reproduces the data quite well, but requires a very precise tuning of the parameters determining $G_{N/A}$ and nucleonic form factor.

3.6. S aszel, Rożynek and Wilk [16]

The idea of an effective nucleon mass being smaller than the physical one was exploited earlier by Staszel, Rożynek and Wilk [16]. They introduced x-dependent mass $M^*(x) = M_{free}/(1-\kappa(1-x))$; where κ is a fitted parameter.

This leads to the following expression for the structure function:

$$F_2^A(x) = \frac{c(1-\kappa)}{[1-\kappa(1-x)]^2} F_2\left(\frac{x}{1-\kappa(1-x)}\right). \tag{15}$$

This formula does not include the motion of the nucleon inside nucleus. One obtains the full expression for the F_2^A in a similar fashion as in formula (13). Such prescription allows one to get a good description of the data.

The authors have also pointed out the connection between the decrease of (effective) nucleon mass and the increase of confinement radius inside nucleus.

3.7. Llewellyn Smith, Ericson and Thomas [13–14]

Another point of view on the description of a nucleus is presented in a model proposed by Llewellyn Smith [13] and developed by Ericson and Thomas [14]. They take into account that the nuclear matter contains pions in addition to neutrons and protons. Therefore one has to take into account DIS of a lepton on a pion as well as on a nucleon (diagram in Fig. 2). This leads to the additional pionic contribution to the structure function:

$$\delta F_2^A = \int_{x/A}^{1} f_\pi(z) F_2^\pi(x/zA, Q^2) dz, \tag{16}$$

where $f_\pi(z)$ is the probability (per nucleon) of finding a pion carrying momentum fraction of a nucleon between z and $z+dz$. This function can be calculated in a standard nuclear model in terms of spin-isospin response function R_π [27] or nuclear wave function [28]. This extra pionic contribution turns out to reproduce accurately the enhancement of F_{2A} at small x [14]. Depletion at large x is obtained by assumption that momentum fraction carried by quarks in nucleus is the same as in free nucleons [13]. This modifies the distribution of nucleons inside nucleus so as to satisfy nucleon number and momentum sum rule.

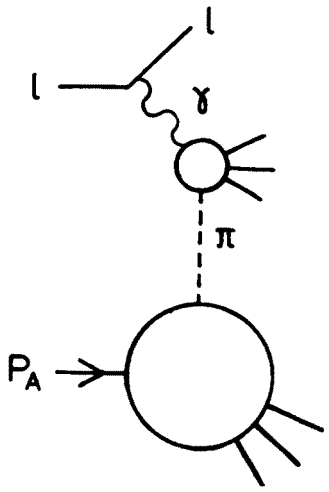

Fig. 2. Pionic contribution to the deep inelastic scattering of a lepton from nuclear target

3.8. Titov [15]

In this model [15] Titov takes both multiquark states and mesonic degrees of freedom into account. The author states that according to experimental results on the "cumulative" particle production in hadron-nucleus [29] and lepton-nucleus collisions at large momentum transfer or the data on the deuteron charge formfactor at large Q^2 [30] there is a finite probability of finding a multiquark states inside nucleus. From these data he estimates that the probability of finding a 6q-state inside deuterium $P_D = 0.07$ whereas the same probability for heavy nuclei P_A is two times larger. The shape of quark distributions inside these 6q-states is derived from quark counting rules. According to Ref. [15] multiquark states give an account of short-range part of N–N interactions. One has to add pions to take into account long-range forces. The final expression for the structure function reads:

$$F_2^A(x) = (1-P_A)F_2^N(x)+P_A F_2^{6q}(x/2)+\delta F_2^\pi(x), \tag{17}$$

where F_2^{6q} — structure function of 6q-states; δF_2^π — pionic contribution to the structure function.

The pionic contribution is assumed to be important only for heavy nucleons and is neglected in the case of deuterium. We assume that the same formulae hold for quark distributions.

3.9. Kubar, Plaut and Szwed [17–18]

In our previous paper [19] we used delta isobar model [17]. This model was based on the idea that, according to nuclear physics, nucleus is contaminated by the Δ isobars and this changes its structure function. The idea has been pursued in the paper by Kubar, Plaut and Szwed [18]. Their model expresses the "effective" nucleon structure function in terms of nucleon, Δ isobar and pion structure functions:

$$F_2^A(x) = \sum_{\alpha=n,\pi,\Delta} \int f^\alpha(y) F_2^\alpha(x/y)dy, \tag{18}$$

where $f^{\alpha}(y)$ are momentum distribution functions given by nuclear physics and $F_2^{\alpha}(x)$ are "free particle" structure functions given by DIS. Thus, there are not any adjustable parameters.

We extract quark densities from this model using the formula:

$$q^A(x) = \sum_{\alpha=n,\pi,\Delta} \int f^{\alpha}(y) q^{\alpha}(x/y) dy/y. \tag{19}$$

4. *Results*

We have calculated the ratio $R \equiv (d\sigma/dx_2)_{Fe}/(d\sigma/dx_2)_{D_2}$ for π^+ and π^- beam using formula (4) and extracting quark densities from all models described in Section 3. Results of our calculations are drawn in Fig. 3–6.

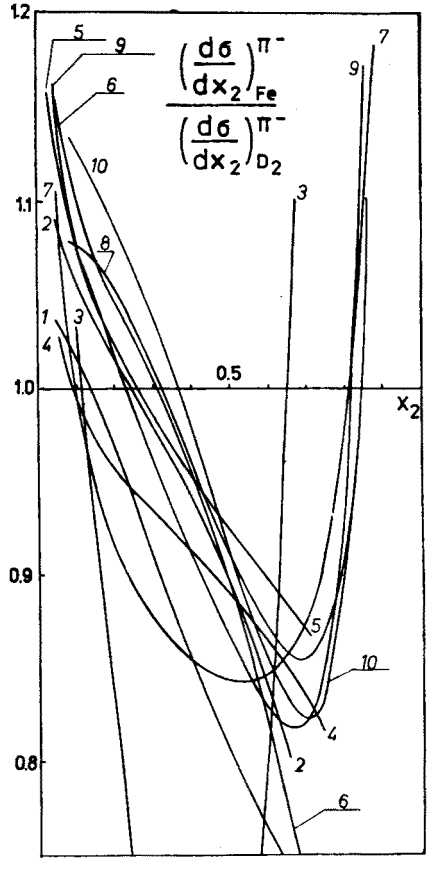

Fig. 3

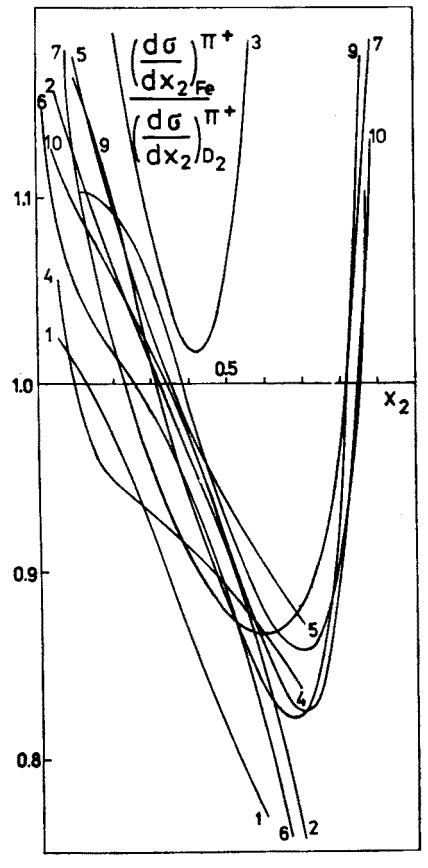

Fig. 4

Fig. 3. Ratio R^{π^-} (as defined in (4)) for an isoscalar target vs x_2. Curves are denoted by numbers corresponding to the different models as follows: *1* — Staszel, Rożynek and Wilk [16], *2* — Levin and Ryskin [9], *3* — Furmański and Krzywicki [4], *4* — Close, Jaffe, Roberts and Ross [7–8], *5* — Szwed [17], *6* — Kubar, Plaut and Szwed [18], *7* — Titov [15], *8* — Dias de Deus [10], *9* — Ericson and Thomas [14], *10* — Dominguez, Morley and Schmidt [12]

Fig. 4. Ratio R^{π^+} for an isoscalar target vs x_2. Curves denoted as in Fig. 1

We wanted to eliminate differences between the models which arise from different parametrisation of structure functions. Thus, where it was possible we used NA3 quark densities [31], re-fitting the parameters of the models to get the agreement with the EMC data. This was done for the models of Ref. [9, 12–14, 17]. For the model of Ref. [8] we used Buras-Gaemers Q^2-dependent structure functions, whereas in the case of the other models we used the structure functions as proposed by their authors.

For the models which do not take Fermi motion into account the resulting ratios are drawn for $x < 0.6$-0.7.

Except for the Furmański and Krzywicki model [5] general pattern of all curves is similar and agrees with the one we obtained previously [19]. Generally the ratio R for π^+ beam is larger than that for π^- beam. For small x the ratio is larger than unity and falls down

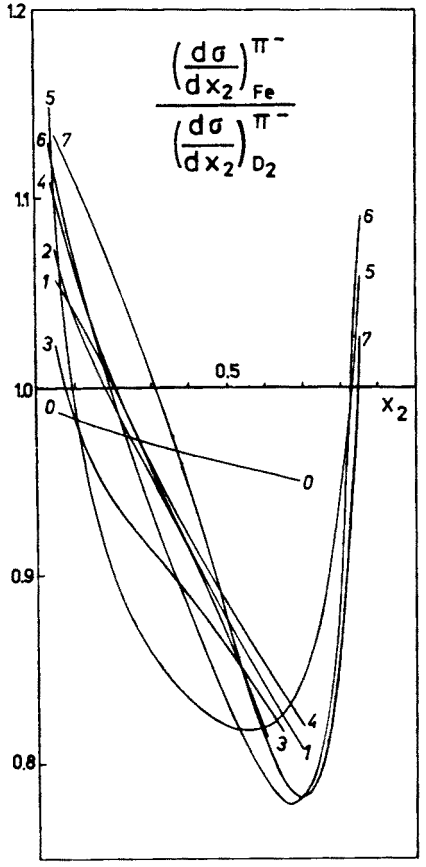

Fig. 5

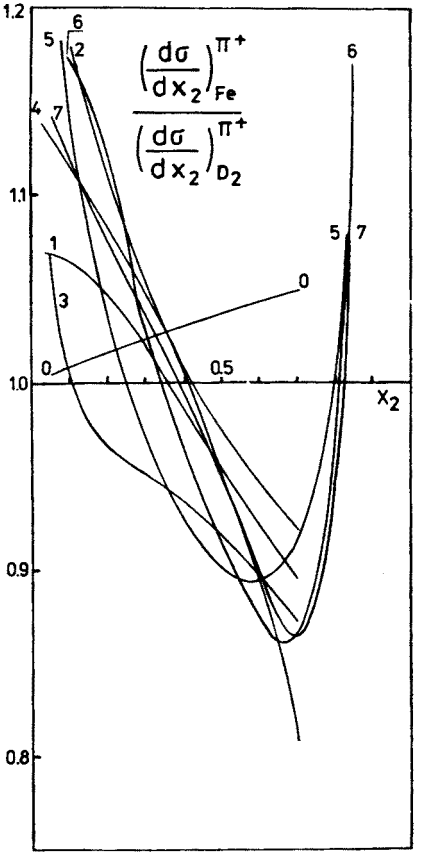

Fig. 6

Fig. 5. Ratio R^{π^-} vs x_2 for a non-isoscalar target. Curves corresponding to the different models are denoted as follows: *0* — no nuclear effects, neutron excess only, *1* — Staszel, Rożynek and Wilk [16], *2* — Levin and Ryskin [9], *3* — Close, Jaffe, Roberts and Ross [7–8], *4* — Szwed [17], *5* — Titov [15], *6* — Ericson and Thomas [14], *7* — Dominguez, Morley and Schmidt [12]

Fig. 6. Ratio R^{π^+} vs x_2 for a non-isoscalar target. Curves denoted as in Fig. 5

with x. For the models with built-in Fermi motion [10, 12, 15] the ratio rises steeply for $x > 0.7$. Qualitatively this curve is similar to the EMC curve. Any model which attempts to explain the EMC effect predicts visible changes in the ratio of Drell-Yan cross section as compared to the naive additive model. The magnitude of this effect is about $\pm 15\%$. Though the predictions of different models do not look exactly the same one must remember that their plots in the case of EMC are different too. If we restrain ourselves to the models which reproduce the EMC data comparatively well, than we see that their predictions for Drell-Yan cross section do not differ very much.

In Fig. 7–8 the ratios $(d\sigma/dx_2)_A^{\pi^+}/(d\sigma/dx_2)_A^{\pi^-}$ for the isoscalar and non-isoscalar target are plotted. Here the discrepancies among the models are even smaller and do not differ significantly from the ones obtained using "free" quark densities. Therefore this measure-

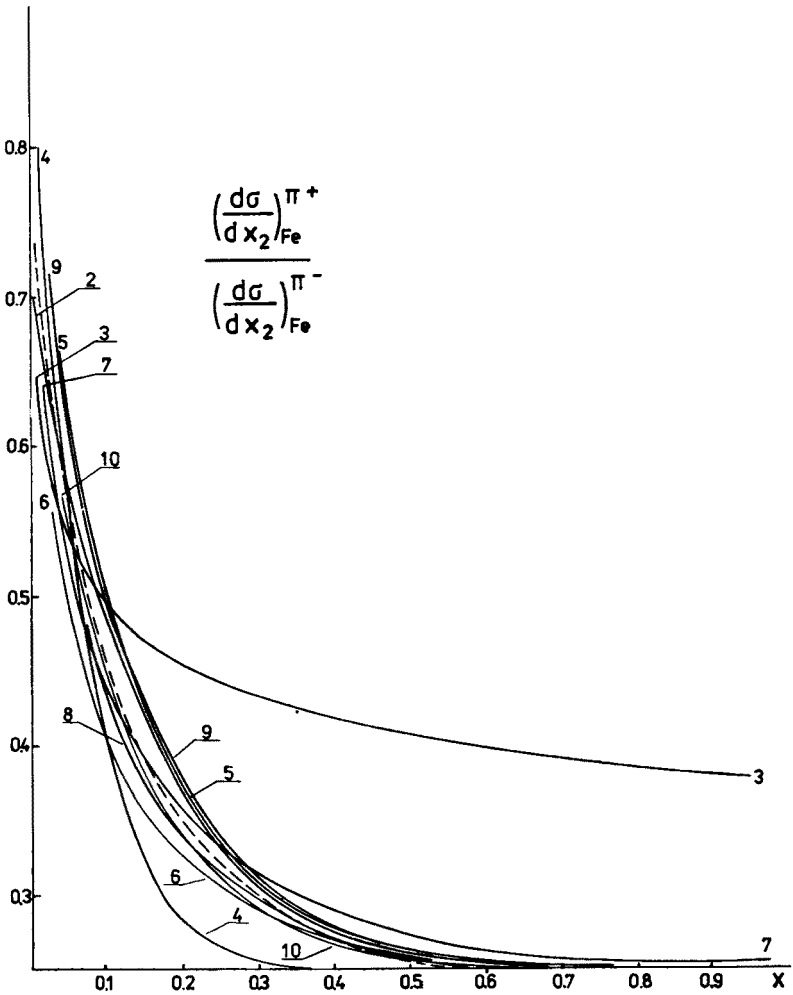

Fig. 7. Ratio $(d\sigma/dx_2)^{\pi^+}/(d\sigma/dx_2)^{\pi^-}$ vs x_2 for an isoscalar target. Curves denoted as in Fig. 3. Dashed line corresponds to the case of "free" nucleons — no nuclear effects

ment (and subsequently $(d\sigma/dm)^{\pi^+}/(d\sigma/dm)^{\pi^-} \sim m^2$, which agrees with the naive Drell-Yan model [32]) will not invalidate any of the models.

In order to compare the predictions of different models with available experimental data [33] we draw the ratio $(d\sigma/dx_2)^{\pi^-}_{H_2}/(d\sigma/dx_2)^{\pi^+}_{Pt} \sim x_2$ (Fig. 9). We assume that the parameters for the platinum target are the same as for the iron one. Because the hydrogen target is not isoscalar, we were able to plot the curves only for the models which allow for non-isoscalarity. Due to large experimental errors it is impossible to rule out any of the models, at least using this data.

We draw also valence quark distributions corresponding to all models (Fig. 10). They do not differ significantly.

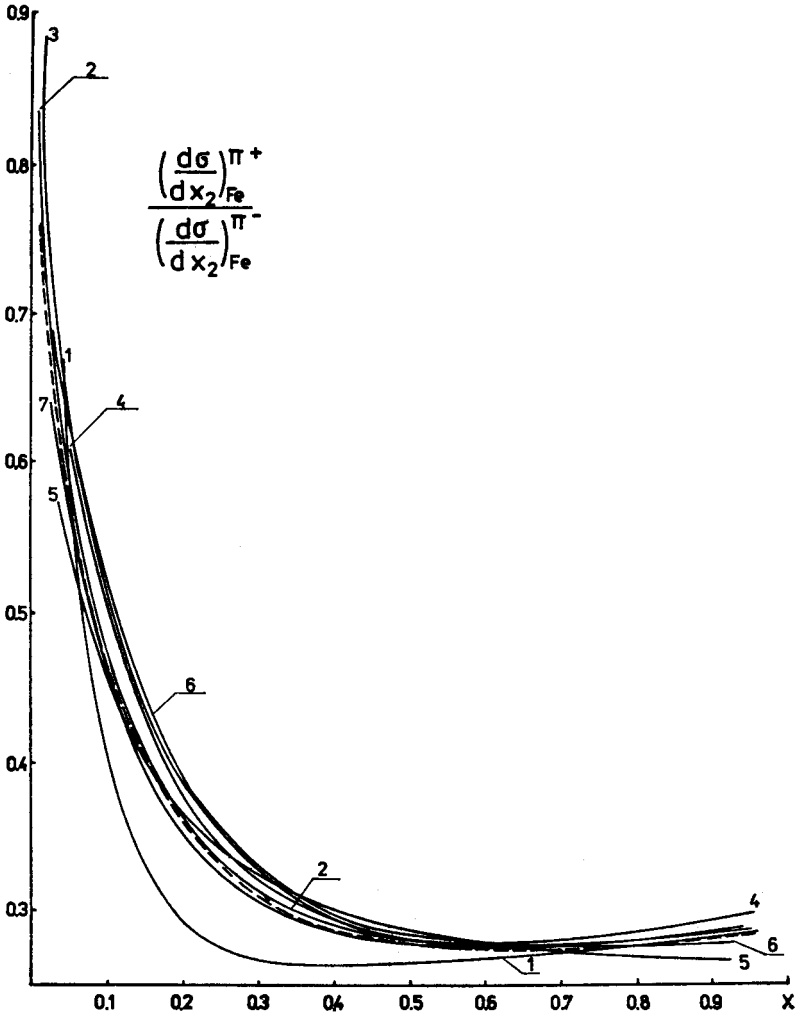

Fig. 8. Ratio $(d\sigma/dx_2)^{\pi^+}_{Fe}/(d\sigma/dx_2)^{\pi^-}_{Fe}$ vs x_2 for a non-isoscalar target. Curves denoted as in Fig. 5. Dashed line corresponds to the case of "free" nucleons — only effects of non-isoscalarity included

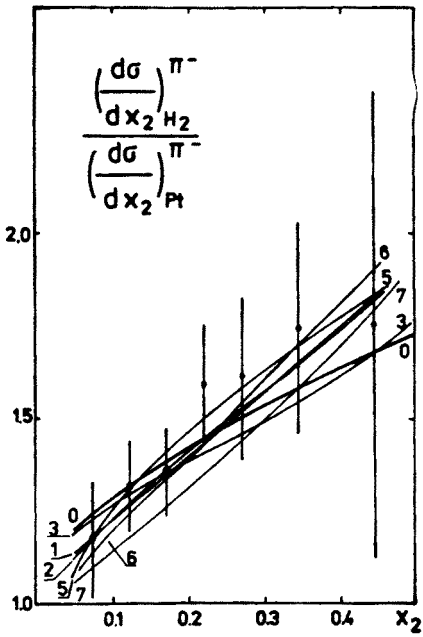

Fig. 9. Ratio $(d\sigma/dx_2)^{\pi^-}_{H_2}/(d\sigma/dx_2)^{\pi^-}_{Pt}$ vs x_2. Experimental data are taken from the NA3 experiment [31]. Curves denoted as in Fig. 5

5. *Conclusions*

We have analysed the effects of changes in quark distributions inside nucleus, as given by different models explaining the EMC effect, on the pion induced Drell-Yan process on nuclear targets. Our results can be summarised as follows:

1. There is an observable effect in the $(d\sigma/dx_2)^{\pi^+}_A/(d\sigma/dx_2)^{\pi^+}_D$ ratio. The effect is predicted by all models and its magnitude ranges from $+15 \div 20\%$ for low x to -15% for intermediate $(0.6 \div 0.7)$ x.

2. Models, which reproduce the EMC data, give predictions for the Drell-Yan process which are similar to one another. Differences among these predictions are small and therefore difficult to measure. Thus the Drell-Yan process cannot be used as a test which differentiates one model from another.

3. Valence quark distribution functions extracted from different models (Fig. 10) look alike, although they are calculated basing on different principles.

4. The fact that different models predict qualitatively the same behaviour of Drell-Yan cross sections seems to support the idea that the sufficiently accurate measurement of the ratio of Drell-Yan cross sections will visibly differ from unity.

We would like to thank Professor A. Białas for his help and encouragement. One of us (K.J.H.) would also like to thank M. Staszel, J. Rożynek and G. Wilk for useful discussions.

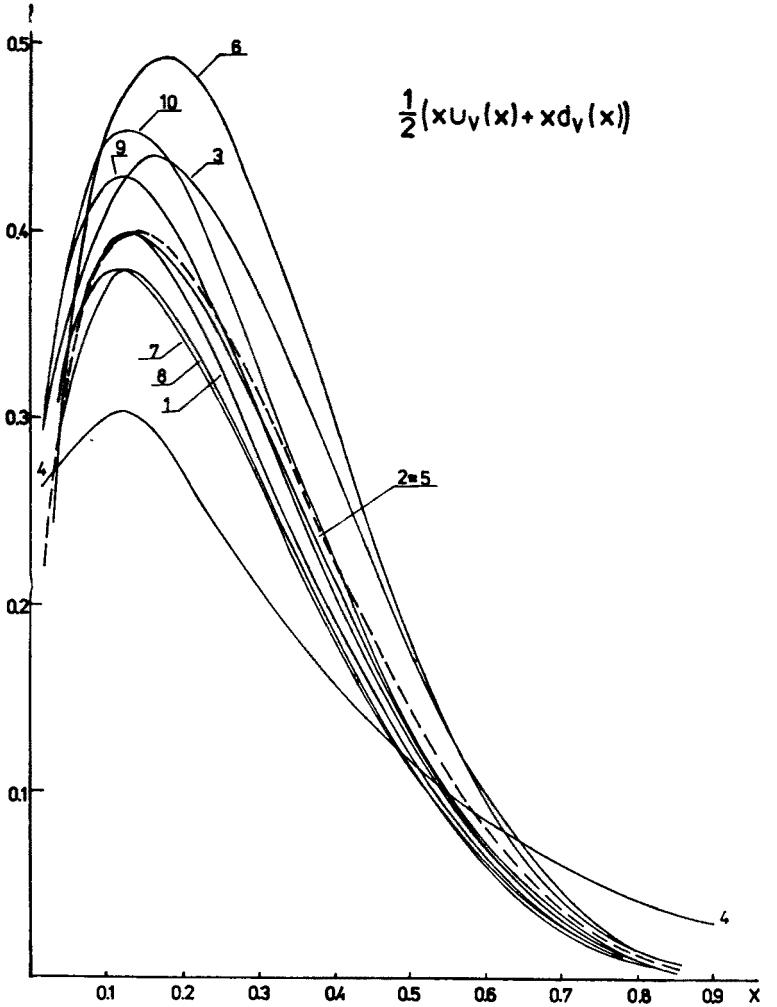

Fig. 10. Valence quark distributions for an isoscalar target vs x as predicted by different models. Curves denoted as in Fig. 3. Dashed line denotes "free" NA3 valence quark distribution

REFERENCES

[1] J. Aubert et al., *Phys. Lett.* **123B**, 107 (1983).
[2] A. Bodek et al., *Phys. Rev. Lett.* **51**, 534 (1983).
[3] A. Bodek et al., preprint SLAC — PUB — 3257, November 1983.
[4] A. Krzywicki, *Phys. Rev.* **D14**, 152 (1976).
[5] W. Furmański, A. Krzywicki, Orsay preprint LPTHE Orsay 83/11 (1983).
[6] R. L. Jaffe, *Phys. Rev. Lett.* **50**, 228 (1983).
[7] F. E. Close, R. G. Roberts, G. G. Ross, *Phys. Lett.* **129B**, 346 (1983).
[8] F. E. Close, R. L. Jaffe, R. G. Roberts, G. G. Ross, *Phys. Lett.* **134B**, 449 (1984).
[9] E. Levin, M. Ryskin, Leningrad preprint 888, August 1983.
[10] J. Dias de Deus, Munich preprint MPI-PAE/PTh 61/83 (1983); and Lisboa preprint CFMC E-1/84 (1984).

[11] L. Kondratyuk, M. Shmatikov, Moscow preprint ITEP 84-13 (1983); G. Cohen-Tannoudji, H. Navelet, CEN-Saclay preprint SPhT-83-97 (1983); H. Pirner, J. Vary, Heidelberg preprint UNI-HD-83-02 (1983); S. Date, *Progr. Theor. Phys.* **70**, 1682 (1983); H. Faissner, B. Kim, *Phys. Lett.* **130B**, 321 (1983); M. Chemtob, R. Peschanski, CEN-Saclay preprint SPhT-83-116 (1983); B. Clark, S. Hama, B. Mulligan, K. Tamaka, Ohio preprint DOE-ER-01545-341 (1984).
[12] C. A. Dominguez, P. D. Morley, I. A. Schmidt, Valparaiso preprint USM-TH-19 (1984).
[13] C. M. Llewellyn Smith, *Phys. Lett.* **128B**, 107 (1983).
[14] M. Ericson, A. W. Thomas, *Phys. Lett.* **128B**, 112 (1983).
[15] A. Titov, Dubna preprint E2-83-460 (1983).
[16] M. Staszel, J. Rożynek, G. Wilk, *Phys. Rev.* **D29**, 2638 (1984).
[17] J. Szwed, *Phys. Lett.* **128B**, 245 (1983).
[18] J. Kubar, G. Plaut, J. Szwed, Nice preprint NTH 84/1 (1984).
[19] T. Chmaj, K. J. Heller, *Acta Phys. Pol.* **B15**, 473 (1984).
[20] S. D. Drell, T. M. Yan, *Phys. Rev. Lett.* **25**, 316 (1970); for a reviev see R. Stroynowski, *Phys. Rep.* **71**, 1 (1981); F. Vanucci, *Acta Phys. Pol.* **B12**, 21 (1981) and also I. R. Kenyon, CERN preprint CERN/EP 82-81.
[21] R. F. Peierls, T. L. Trueman, L. L. Wang, *Phys. Rev.* **D16**, 1397 (1977).
[22] C. T. Sachrajda, SLAC preprint SLAC — PUB — 3181, August 1983.
[23] J. Kubar, M. Le Bellac, J. L. Meunier, G. Plaut, *Nucl. Phys.* **B175**, 251 (1979).
[24] See experimental results of Ref. [33] and also S. Falciano et al., *Phys. Lett.* **104B**, 416 (1981); K. J. Anderson et al., *Phys. Rev. Lett.* **42**, 944 (1979).
[25] J. Kuti, V. Weisskopf, *Phys. Rev.* **D4**, 348 (1971).
[26] I. A. Schmidt, R. Blankenbecler, *Phys. Rev.* **D16**, 1318 (1977); *Phys. Rev.* **D15**, 3321 (1977).
[27] M. Ericson, E. Oset, H. Toki, M. Weise, *Phys. Rep.* **83**, 81 (1982).
[28] B. L. Friman, V. R. Pandharipanda, R. B. Wiringa, *Phys. Rev. Lett.* **51**, 763 (1983).
[29] A. M. Baldin, *Particles and Nuclei* **8**, 429 (1977).
[30] A. P. Kobushkin, *Sov. J. Nucl. Phys.* **28**, 495 (1978); V. V. Burov et al., *Z. Phys. A — Atoms and Nuclei* **306**, 1491 (1982); I. T. Obuklovsky, E. V. Tkalya, *Sov. J. Nucl. Phys.* **35**, 288 (1982).
[31] J. Badier et al., CERN preprint CERN/EP 80-150 (1980).
[32] J. Badier et al., CERN preprint CERN/EP 79-137 (1979).
[33] J. Badier et al., *Phys. Lett.* **104B**, 335 (1981).